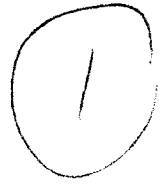


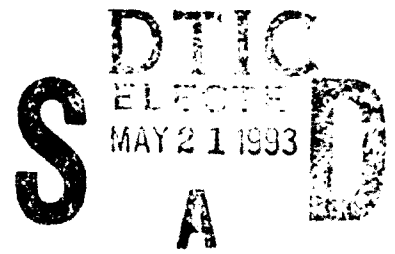
AD-A264 670



AGARD

ADVISORY GROUP FOR AEROSPACE RESEARCH & DEVELOPMENT
7 RUE ANCELLE 92200 NEUILLY SUR SEINE FRANCE

**Paper Reprinted from
AGARD Conference Proceedings 528**

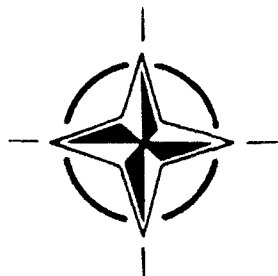


Radiolocation Techniques

(Les Techniques de Radiolocalisation)

93 80

93-11360



NORTH ATLANTIC TREATY ORGANIZATION

UNCLASSIFIED

21a NAME OF HEADQUARTERS OR OFFICE R. B. Rose	21b TELEPHONE NUMBER (Include Area Code) (619) 553-3069	21c MAILING CODE Code 512

Approved For	
NTIS - CS/NI	✓
DTIC TAB	✓
Unannounced	✓
Justification	
by	
Distribution	
Date of this report	
Date	For Distribution
A-1	20

RADIOLOCATION OF A SATELLITE-BORNE LOVHF BEACON

Robert B. Rose
Ionospheric Branch, Code 542
Ocean and Atmospheric Sciences Division
Naval Command, Control Ocean Surveillance Center, RDT&E Division
San Diego, CA, 92152-5000, USA

ABSTRACT

A year long experimental program was conducted to measure refractive bending, or how much the signal deviates from true line of sight, at low VHF frequencies (29.5 MHz), and to determine whether this deviation or error could be predicted using large scale ionospheric models such as the Ionospheric Conductivity and Electron Density (ICED) program. An experiment to directly measure the angle of arrival of a 29.5 MHz signal from an orbiting satellite was successfully completed. The satellite was in a circular orbit at an altitude of 1000 km. It was shown that refractive errors can be directly related to the electron density along the measurement slant range. Ionospheric disturbances such as sporadic E and ionospheric storms produce large, short term errors that can approach 10 degrees. In addition to day/night variations, seasonal and solar cycle sensitivities were found. The refractive error varied so rapidly with respect to time and space that its prediction with a median value ionospheric code is almost impossible.

INTRODUCTION

Recent advances in the science of ionospheric measurement provide a detailed picture of how the ionosphere is structured with respect to time and space. What is seen is a much more turbulent plasma than previously recognized, one that is very susceptible to changes in solar radiation patterns and the earth's magnetic field. This new knowledge raises questions about the predictability of ionospheric structure. The bulk of the models used to predict electron density between 50 km and 1000 km are based on empirical measurements. Their outputs are median values. The key concern is how well they typify the real-time ionosphere as a function of time of day, season and geographical location.

Programs at this facility use a variety of ionospheric models. Usually, the first question asked is how well they can replicate the dynamics of the real world ionosphere. Recently this question was posed about the Ionospheric Conductivity and Electron Density (ICED) model (Daniell, et al., 1986). The application of interest required an accurate prediction of the electron density between the ground and outer space. One output from ICED is a true height electron density profile between 50 and 1000 km. A predicted total electron content (TEC) was derived from this. The

challenge was to design an experiment that would measure TEC, or something equivalent, to test ICED model profiles.

The discovery of an orbiting satellite system that carried a low VHF (LoVHF) beacon operating at 29.5 MHz suggested a novel approach to this problem. The remainder of this paper describes an experimental program in which a ground based HF interferometer was used to locate and track the LoVHF beacon as it passed overhead. The objective of this experiment was to (1) directly measure the refractive error, or how much the signal deviates from true line of sight, on the transionospheric signal; (2) determine the magnitude and characteristics of this uncorrected error; and (3) develop an electron density data base against which the ICED model could be compared.

EXPERIMENTAL METHOD

The signal source for this experiment was a low orbiting satellite. It contained several HF/LoVHF beacons and transponders which produced morse code signals at 29.5 MHz. For this project, the morse beacons were used as point signal sources. Originally planned as two individually orbiting platforms, the satellites were launched together on a navigational satellite (NAVSAT). This was fortunate as the NAVSAT was maintained in an accurate circular orbit at 1000 kilometer altitude. This encompasses 98 percent of the ionosphere. The satellite's orbital inclination of 83 degrees provided two or three useful passes a day. Data were collected every 15 seconds as long as the 29.5 MHz beacon signal strength was sufficient for gathering data. A normal pass would last 12-13 minutes from horizon to horizon.

Conceptually, the experiment was simple. The "apparent" position of the satellite was measured and compared to the "real" position derived from predicted ephemeris data specifying the orbital location of the satellite in space and time. The difference, expressed in angular error in degrees, is the refractive bending error caused by the ionosphere between the satellite and the ground station. The electron density was then derived using coefficients of refraction at the beacon frequency.

To measure the satellite-borne beacons, a direction finder with fast processing time was required. It had to make high time-resolution measurements of angle of arrival (AOA) in azimuth and elevation. At that time, the only system capable of accomplishing this was a Single Site Locating (SSL) Testbed at Southwest

Research Institute (SWRI) in San Antonio, Texas. The system, described earlier (Rose, 1992), is a 7 element interferometer which uses an "L" shaped array. It can perform successive angle of arrival measurements in 3.5 millisecond intervals. At this sampling rate errors due to satellite motion are effectively minimized.

In order to perform the desired comparisons with ionospheric models, the refractive bending data had to be expressed in terms of electron density. Before and after each pass, the peak electron density was measured with a vertical incidence sounder. The measured F-region critical frequency, the foF2, is directly related to peak electron density (Ne) by:

$$(1) \quad Ne(\text{el/cm}^3) = 1.24 \times 10^4 \times \text{foF2}(\text{MHz})$$

Because the interferometer produced large amounts of data very quickly, data collection periods were limited to windows that were four seconds in length. In this time 1152 frames of data were collected. A frame is a 3.5 millisecond AOA measurement of the phase data from each of the seven interferometer elements. The satellite moved approximately 30 km during the 4 second window or about 26 meters between frames. Each frame was time tagged and stored on magnetic media. In addition, a vertical incidence sounder ionogram was made prior to and after each pass to determine ionospheric conditions. Next, each frame underwent phase linearity testing. This test determines whether the array observed a plane-wave and made an AOA observation based on one signal. The frames that passed this test, typically 100-500 of the 1152 collected in each window, were put into an analysis file for further processing. Figure 1 shows an analysis file segment from one four second window. In a final step, the data are reduced into spreadsheet format for analysis.

DISCUSSION OF THE DATA

The experimental program was conducted between October 1988 and December 1989. Over this period, 217 passes provided information that were suitable for analysis. These included:

- 28 Cases - Setup/Calibration - (October - December 1988)
- 40 Cases - Winter- (January - March 1989)
- 40 Cases - Spring (April - June 1989)
- 50 Cases - Summer - (July - September 1989)
- 52 Cases - Fall (October - December 1989)

This experiment performed above expectations throughout the year. There was no period in which data could not be acquired.

A unique aspect of this experiment was the amount of the ionosphere that was measured on each pass. Depending on how

SWRI SATELLITE DATA FILE
DAY # 171 DATA FILE A

TIME HH:MM:SS.SS	TRUE		SLANT RANGE	OBSERVED		DELTA	
	AZ	EL		AZ	EL	AZ	EL
03:55:46.00	47.2	42.4	1365	47.5	42.9	0.1	-0.5
03:55:46.01	47.2	42.4	1365	47.7	42.6	0.5	-0.2
03:55:46.02	47.2	42.4	1365	47.2	42.9	0.0	-0.5
03:55:46.03	47.2	42.4	1365	48.1	42.7	-0.9	-0.1
03:55:46.04	47.2	42.4	1365	47.9	42.5	-0.7	-0.1
03:55:46.05	47.2	42.4	1365	47.3	42.7	-0.1	-0.1
03:55:46.06	47.2	42.4	1365	47.5	42.4	-0.3	0.0
03:55:46.08	47.2	42.4	1365	48.0	42.7	-0.8	-0.3
03:55:46.09	47.2	42.4	1365	47.6	42.8	-0.4	-0.4
03:55:46.10	47.2	42.4	1365	47.4	43.2	-0.2	-0.8
03:55:46.12	47.2	42.4	1365	46.9	42.6	0.3	-0.2
03:55:46.30	47.1	42.3	1366	47.0	42.9	0.1	-0.6
03:55:46.31	47.1	42.3	1366	47.4	43.0	-0.3	-0.7
03:55:46.33	47.1	42.3	1366	47.3	42.7	-0.2	-0.4
03:55:46.34	47.1	42.3	1366	47.4	42.6	-0.3	-0.3
03:55:46.35	47.1	42.3	1366	47.4	42.6	-0.3	-0.3
03:55:46.36	47.1	42.3	1366	47.6	42.8	-0.5	-0.5
03:55:46.37	47.1	42.3	1366	47.6	42.7	-0.5	-0.4
03:55:46.38	47.1	42.3	1366	47.5	42.4	-0.4	-0.1
03:55:46.39	47.1	42.3	1366	47.2	42.8	-0.1	-0.5
03:55:46.42	47.1	42.3	1366	47.0	42.6	0.1	-0.3
03:55:46.43	47.1	42.3	1366	47.6	42.8	-0.5	-0.5
03:55:46.44	47.1	42.3	1366	47.2	42.5	-0.1	-0.2
03:55:46.53	47.1	42.3	1367	47.0	42.8	0.1	-0.5
03:55:46.54	47.1	42.3	1367	47.0	42.8	0.1	-0.5
03:55:46.55	47.1	42.3	1367	47.7	42.7	-0.6	-0.4
03:55:46.56	47.1	42.3	1367	47.6	42.9	-0.5	-0.6
03:55:46.57	47.0	42.3	1367	47.7	42.5	-0.7	-0.2
03:55:46.58	47.0	42.3	1367	47.3	42.8	-0.3	-0.5
03:55:46.59	47.0	42.3	1367	47.2	42.8	-0.2	-0.5
03:55:46.60	47.0	42.3	1367	47.1	42.0	-0.1	0.3
03:55:46.61	47.0	42.3	1367	47.2	42.9	-0.2	-0.6
03:55:46.63	47.0	42.3	1367	47.2	42.9	-0.2	-0.6
03:55:46.64	47.0	42.3	1367	47.7	43.0	-0.7	-0.7
03:55:46.65	47.0	42.3	1367	46.9	42.6	0.1	-0.3
03:55:46.66	47.0	42.3	1367	47.0	42.8	0.0	-0.5
03:55:46.67	47.0	42.3	1367	47.4	42.8	-0.4	-0.5
03:55:46.73	47.0	42.3	1367	47.3	42.4	-0.3	-0.1
03:55:46.75	47.0	42.3	1367	47.9	42.6	-0.9	-0.3
03:55:46.77	47.0	42.3	1367	47.0	42.7	0.0	-0.4
03:55:46.78	47.0	42.3	1367	47.2	43.0	-0.2	-0.7
03:55:46.80	47.0	42.3	1368	47.1	42.7	-0.1	-0.4

Figure 1 - Segment of phase linear data from a four second frame

close the satellite passed overhead to the receiver, the data mapped represented an area about 600 km wide and several thousand kilometers long. The predicted ephemeris data were checked on each pass by carefully observing the times of acquisition of signal (AOS) and loss of signal (LOS). This normally occurs as the satellite comes over the horizon and is in line of sight of the receiving station. Any error in the predicted ephemeris data showed up as a bias in the output data and was easily spotted. AOS on a north to south pass was the most reliable test with the difference between predicted and observed AOS times never exceeding several seconds. Prediction of LOS to the south was completely unreliable, with the differences between predicted and observed being tens of seconds to minutes. This was because the 29.5 MHz signal would become a skywave signal at low elevation angles and could be heard half way around the world.

Most of the data were collected between elevation angles of 20 and 82 degrees. Below 20 degrees, the slant ranges exceed 2000 km, the signal to noise is very poor and the likelihood of an undistorted plane wave signal was very low. Directly overhead above 82 degrees, the arctangent calculation in the azimuth calculation breaks down and answers are unreliable. Once these boundaries were established, data collection became straight forward.

Several trends appeared early in the tests and it soon became easy for the

analyst to discern whether the pass was north to south or vice versa. The large patches of irregularities that characterize latitudes below 30 degrees north were evident. The ionosphere to the north of the receiver site was less dense than to the south. Changes in signals from the north were orderly and at expected levels. Signals from the south were always variable and unpredictable with greater errors at long slant ranges.

Because of the satellite's orbit, the times signals could be received changed daily. This allowed a measurement schedule that could probe the ionosphere at different times of day and night. The periods at pre-sunrise (electron density minimum) and pre-sunset (electron density maximum) were always the most interesting. At pre-sunrise in the winter, the electron density almost disappears allowing the scientist to determine the baseline accuracy of the interferometer without interference from the ionosphere.

Figure 2(a) shows a pass that occurred during the winter at pre-sunrise (absolute minimum electron density). To the north, there is little error in either azimuth or elevation angles that are measured. For this pass, the overall miss-distance error between predicted and observed AOA is 1.5%. Numerous other passes that occurred during the pre-sunrise period show about the same accuracy. Therefore, this is close to the minimum error of the SSL.

Figure 2(b) shows a summer pre-sunset case. The refractive error is largely effected by slant range, increasing as ranges increase. The average overall AOA error is 3.5%. However, as range increases, the error exceeds 5%, similar to the accuracies of the SSL in locating terrestrial targets.

Figure 3 shows the effects of seasonal changes and how refractive error changes with season. Figure 3(a) depicts winter night where error is minimal due to lower electron density. Even at night there is some evidence of the differences in the ionosphere to the north and the south. Figure 3(b) shows what happens during the night in the summer when electron density is greater. In both cases the data were collected during pre-sunrise when electron density is lowest.

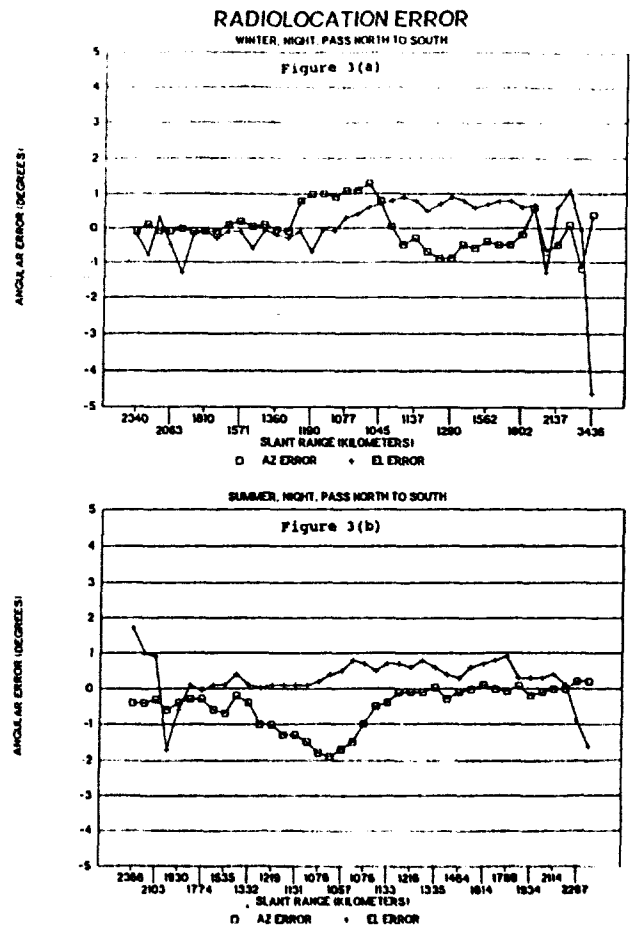
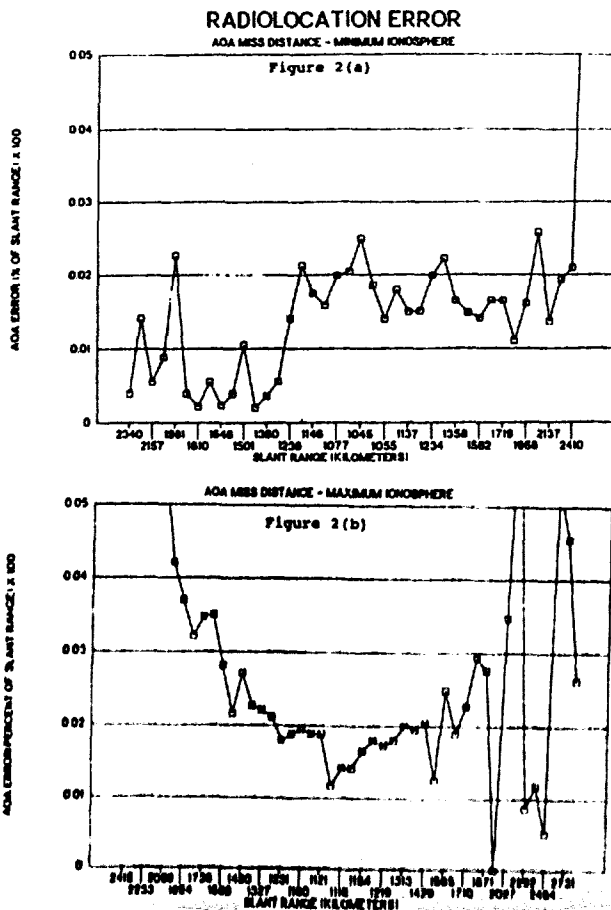
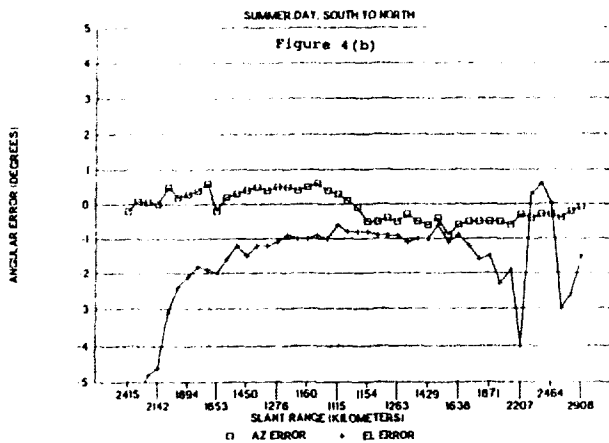
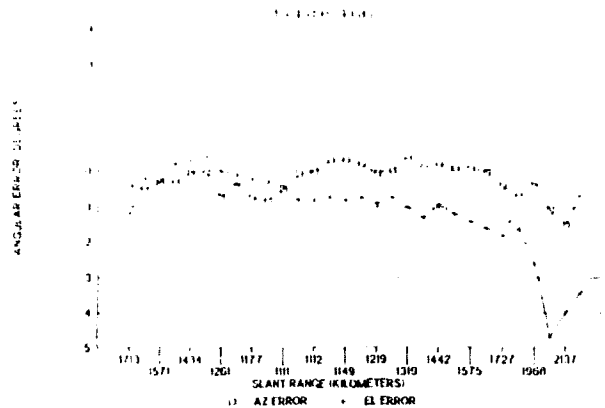


Figure 4 shows the effect of season on refractive error during daylight when electron density is at maximum values. The largest difference is in elevation angle error. In figure 4(a), the winter day, there is little refractive bending until the signal source is well south of the receiver site, and the errors are less than one degree. In figure 4(b), the summer day, there is a more pronounced signal bending over the longer slant ranges. For both examples the point of closest approach is nearly the same and at that point the errors are nearly the same.

RADIOLATION ERROR

EFFECTS OF INTENSE SPORADIC E



Analysis of the individual spreadsheet data for each pass showed that the errors in the elevation angle were the primary contributor to the overall error. Elevation errors are caused by horizontal electron density gradients which, in turn, are caused by cyclic changes in time of day, season, and solar cycle. These changes are smoother and less radical than those caused by vertical gradients.

Vertical gradients cause errors in the azimuth angle of arrival. These tend to be caused by short term phenomena such as sporadic-E, traveling ionospheric disturbances and ionospheric storm effects. Figure 5 shows the effect of sporadic E on a summer morning pass. The positive shift in azimuth error when the satellite is nearest the receiver (1101 km) is due to the very intense overhead E region. As the signal source moves away, the effects diminish rapidly because the layer is relatively thin.

After a year of making measurements, there was sufficient data to observe the diurnal and seasonal ionospheric effects on AOA measurements. Each pass was reduced to a composite vector sum of the elevation and azimuth errors as a function of foF2. This was then plotted by season (Figure 6). While the results shown in figure 6 are not surprising, it does provide a quantitative relationship that can be used to test computer simulations.

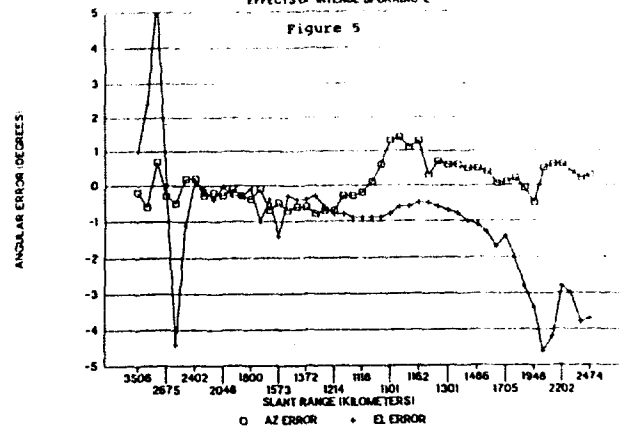
The deviation of the summer curve from the other three seasons is referred to as the "seasonal anomaly."

The curve in figure 6 indicates that the relationship between transionospheric angular error and electron density is nearly linear. They can be expressed with two terms, one for winter, spring and fall, and one for summer. The measurements were made at solar cycle maximum when electron densities are the highest. Therefore, the relationships for solar minimum are already accounted for because it is already known that one of the effects of solar decline is that foF2 values are less as depicted in the lower half of figure 6. The data in figure 6 represent the "slowly varying" component for modeling transionospheric electron density and the resultant refractive bending.

RADIOLATION ERROR

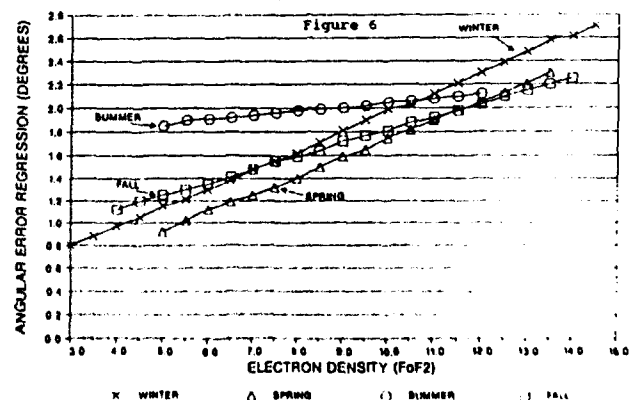
EFFECTS OF INTENSE SPORADIC E

Figure 5



TRANSIONOSPHERIC EXPERIMENT 29.5 (MHZ)

ANGULAR ERROR BY SEASON



With data acquisition complete, the next objective was to compare observed data with predicted data from ICED. For the exact times measurements were made, model ionospheres were derived from ICED. The homing mode of a raytrace program was used to trace the signal ray path from the satellite to some ground point. Ephemeris data on the satellite's location were used as a starting point. The output was the latitude and longitude of the ground intercept point. This was converted into azimuth and elevation error and then

compared to the measured data. One method of displaying the comparisons is shown in figure 7. The differences between observed and predicted azimuth and elevation errors are used to generate a differential azimuth/elevation scatter plot. If the model predictions are close to the actual measured data, then the scatter plot provides a tight cluster about zero. The more the prediction deviates from the observed data, the greater the spreading of the data. Figure 7 shows data comparisons for both day and night situations between elevation angles of 30 and 60 degrees, the optimum angles for the interferometer array.

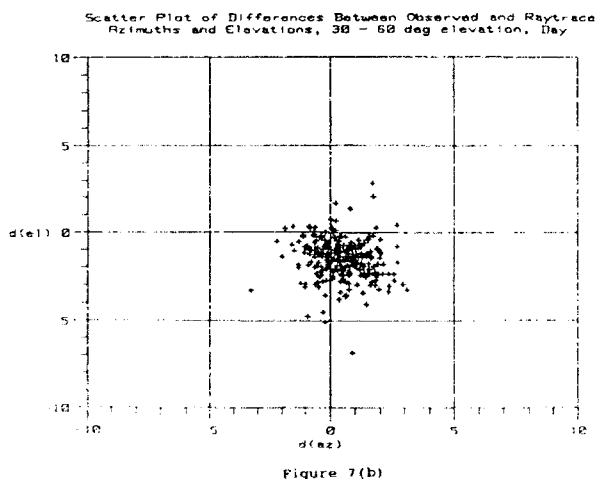
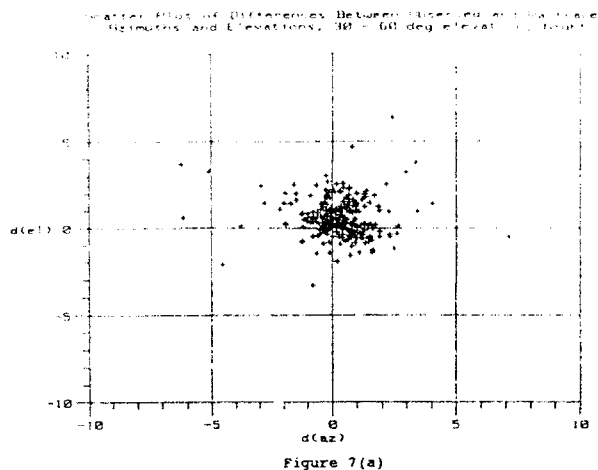


Figure 7(a) represents 246 nighttime data points for true elevation between 30 and 60 degrees. The sample mean elevation difference value is 0.6 degrees with a standard deviation of 1.15 degrees. The mean azimuth difference was 0.25 degrees with a standard deviation of 1.36 degrees. With the minimal night ionosphere the predicted data set does track the observed data set, although with a tendency to under-predict elevation.

In figure 7(b), 269 daytime data points are shown. A fairly tight distribution is seen but the center of the elevation distribution has become negative, indicative of over-prediction. The mean elevation difference is -1.54 degrees with a standard deviation of 1.12

degrees. The mean azimuth error is 0.45 degrees with a 1.0 degree standard deviation. In combination with the results for the nighttime case, these results point to the error being introduced by the ICED model rather than the raytrace. This is because the interpolation scheme used in the raytrace is the same for both night and day.

CONCLUSIONS

A year long campaign successfully produced a unique data base on the refractive bending of a LoVHF signal caused by a variety of ionospheric conditions. A ground-based direction finder used an orbiting beacon on 29.5 MHz to map ionospheric electron density. The effects of day/night cycles and season were observed. Short term variations, such as those due to sporadic E and ionospheric storms were measured.

During periods of electron density minimum, the vector sum of the azimuth and elevation errors ranged near 1.5 percent of the slant range between the satellite and receiver. This is likely the instrumental accuracy of the 7 channel interferometer that was used.

During measurements when the electron density was at maximum values, the transionospheric angular errors ranged between 5 and 10 percent of range. Short term gradients caused by sporadic E and ionospheric storms pushed the errors to excessive levels.

A relationship was developed that relates transionospheric angular error to the peak electron density as measured from a ground-based vertical sounder. This was then used to test various ionospheric models to see if they could first replicate the observed bending and then correct for it. The results were not satisfactory as the ICED model tends to over-predict the electron density during daylight hours. It is suspected that this is due, in part, to a poorly modeled topside ionosphere, from 350 km up to the 1000 kilometer altitude of the satellite.

ACKNOWLEDGEMENT

The author acknowledges the contributions of Richard A. Sprague for innovative analytical work and Dr. David R. Lambert in the review and editing of this paper.

REFERENCES

Daniell Jr., R.E., D.T. Decker, D.N. Anderson, J.R. Jasperse, J.J. Sojka, R.W. Schunk, "A Global Ionospheric Conductivity and Electron Density (ICED) Model," Proceedings from the Ionospheric Effects Symposium, The Effect of the Ionosphere on Radiowave signals and System Performance, 1-3 May 1990

Rose, R.B., "A Current Assessment of Single Site Locating Technology," Electromagnetic Wave Propagation Panel NATO-AGARD 50th Symposium on Radiolocation Techniques, London, UK, 1-5 June 1992.

DISCUSSION

T. COYNE

I understood from your previous presentation (paper 10) that problems above 82° elevation were associated with ionospheric tilts. I take it from your present paper this is not correct. The problem is an instrumental one - which surprises me as you are close to line-of-site to the interferometer when it is equipped with loops.

AUTHOR'S REPLY

For an interferometer, azimuth calculations become unstable at elevation angles of greater than 82°. This is systematic of the system that we are using. A fairly complex solution was developed by Frank Polkinghorn of NRL to circumvent the large azimuth errors at overhead angles.

E. HAYDEN

For the interferometer system in question, when the signal arrives from directly overhead it is true that the azimuth measurement becomes indeterminate. However, in that same situation it is important to keep in mind that the elevation measurement is at its most accurate because the wave direction is normal to the array plane.

AUTHOR'S REPLY

Concur.

L. BERTEL

Calculation of angle errors requires knowledge of the electron density in the vicinity of the satellite; do you take that parameter into account in your simulations? And, if the answer is 'yes', what ionospheric profile do you use?

AUTHOR'S REPLY

Initially we used rather simplistic assumptions in structuring the experiment. The beacon transmitter was at 1000 km altitude. At this altitude, the emitter is above 96-97% of the total electron content. Therefore, we initially assumed, the transmitter and receiver were completely above and below the ionosphere and the bending observed was due to the plasma in between. The ionospheric profiles we used were from ICED for the midlatitude experiment. With the type of day time errors observed, the median ionospheric electron content is too high already. To account for the residual 3-4% of electron content that exists between 1000 and 1500 km would only increase the error.

C. GOUTELARD

Pourquoi n'utilisez-vous pas le modèle de Bent pour la modélisation de l'ionosphère au voisinage du satellite? (suite à la question de Mr Bertel).

Why not use the Bent model for modeling the ionosphere in the vicinity of the satellite? (Follow-up to Mr. Bertel's question).

AUTHOR'S REPLY

Our project was specifically tasked to investigate useability of electron density profiles from ICED. We could have used the same process on any Ne profile from any model. It just wasn't our task on this project.

H. SOICHER

Transionospheric transmissions at 29.5 MHz are occasionally subjected to anomalous propagation conditions (e.g., reflections to receivers from totally different directions). Have you noticed such? Under what circumstances?

AUTHOR'S REPLY

Yes, myself and the scientists at SWRI, where the measurements were made, were very aware of what happens when signals at 29.5 MHz go skywave. One time on a north-south pass, we observed the beacon until it was over Antarctica. To the south, in the summer when the equatorial anomaly was the furthest north we saw many cases where large azimuth and elevation errors occurred. Normally, measurements to the north were well behaved. We have confirmed cases from ionospheric storms, E_s, auroral backscatter, and equatorial E. However, because of the very extensive data base collected during normal conditions, anomalous propagation amounted to a very small percentage of the data.